SUPPORTING INFORMATION

CO_2 Behavior in a Highly Selective Ultramicroporous Framework: Insights from Single-Crystal X-ray Diffraction and Solid-State Nuclear Magnetic Resonance Spectroscopy

Bligh E. Desveaux,[a] Y. T. Angel Wong,[a] Bryan E. G. Lucier,[a] Victor V. Terskikh,[b] Paul D. Boyle,[a] Shan Jiang[a] and Yining Huang[a,*]

[a]*Department of Chemistry, The University of Western Ontario, 1151 Richmond Street, London, Ontario, Canada, N6A 5B7*

[b] *Department of Chemistry, University of Ottawa, 75 Laurier Ave E, Ottawa, Ontario, Canada K1N 6N5*

[*]Corresponding author: Yining Huang (yhuang@uwo.ca)

Webpage: http://publish.uwo.ca/~yhuang/index.htm

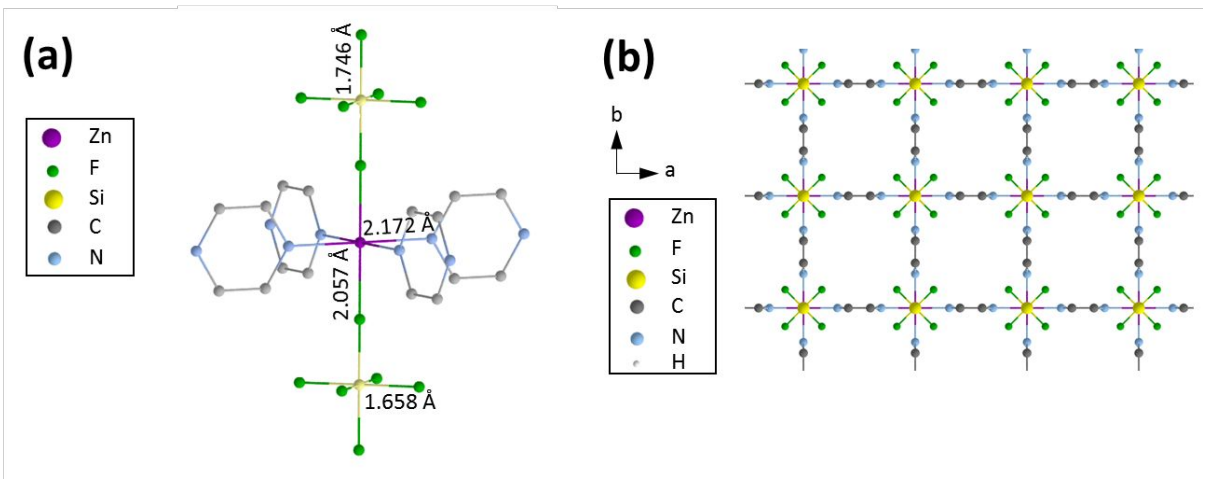

Figure S1. The (a) atomic connectivity and (b) extended crystal structure of as-made SIFSIX-3-Zn at 298 K.[1] Hydrogens are omitted for clarity.

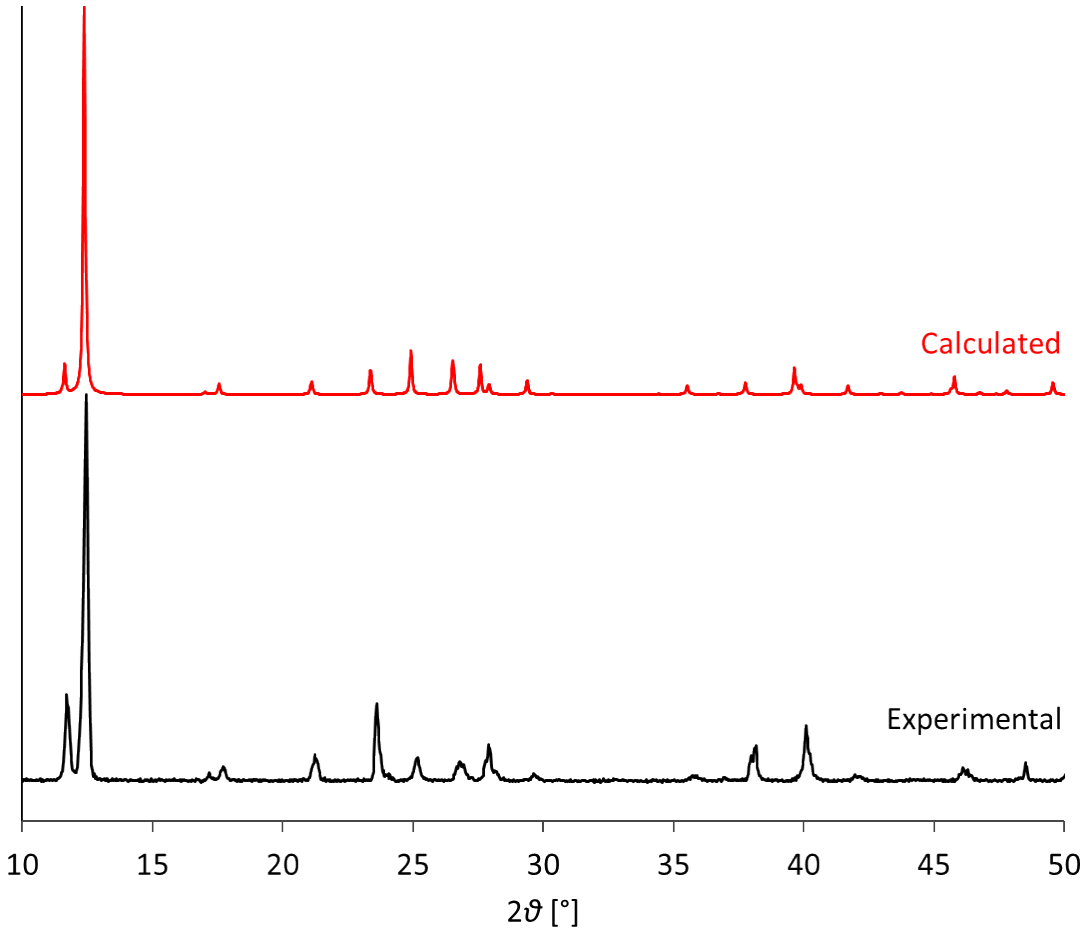

Figure S2. The experimental and simulated pXRD patterns of as-made SIFSIX-3-Zn. The experimental pXRD pattern was collected using CuKα source (λ = 1.5418 Å). The 2θ value was from 5 to 120°. The simulated pXRD pattern was calculated from the reported crystal structure of as-made SIFSIX-3-Zn.[1]

Table S1. A summary of SCXRD data for CO_2-loaded SIFSIX-3-Zn

Formula	$C_{17.86}H_{16}F_{12}N_8O_{3.73}Si_2Zn_2$
Formula Weight (*g/mol*)	817.37
Crystal Dimensions (*mm*)	0.158 × 0.153 × 0.050
Crystal Color and Habit	colourless plate
Crystal System	tetragonal
Space Group	I 4/m c m
Temperature, K	110
a, Å	9.9917(14)
b, Å	9.9917
c, Å	15.088(2)
α,°	90
β,°	90
γ,°	90
V, $Å^3$	1506.3(5)
Number of reflections to determine final unit cell	5046
Min and Max 2θ for cell determination, °	11.74, 131.02
Z	2
F(000)	810
ρ (*g/cm*)	1.802
λ, Å, (CuKα)	1.54178
μ, (cm^{-1})	3.801
Diffractometer Type	Bruker-Nonius KappaCCD Apex2
Scan Type(s)	phi and omega scans
Max 2θ for data collection, °	131.572
Measured fraction of data	0.995
Number of reflections measured	8587
Unique reflections measured	376
R_{merge}	0.0274
Number of reflections included in refinement	376
Cut off Threshold Expression	I > 2sigma(I)

Structure refined using	full matrix least-squares using F^2
Weighting Scheme	$w=1/[sigma^2(Fo^2)+(0.0321P)^2+2.3957 P]$ where $P=(Fo^2+2Fc^2)/3$
Number of parameters in least-squares	39
R_1	0.0209
wR_2	0.0590
R_1 (all data)	0.0225
wR_2 (all data)	0.0605
GOF	1.132
Maximum shift/error	0.000
Min & Max peak heights on final ΔF Map (e^-/Å)	-0.228, 0.270

Where:

$R_1 = \Sigma(|F_o| - |F_c|) / \Sigma F_o$

$wR_2 = [\Sigma(w(F_o^2 - F_c^2)^2) / \Sigma(w F_o^4)]^{½}$

$GOF = [\Sigma(w(F_o^2 - F_c^2)^2) / (\text{No. of reflns. - No. of params.})]^{½}$

Table S2. Atomic coordinates for CO_2-loaded SIFSIX-3-Zn

Atom[a]	x	y	z	$U_{iso/equiv}$
Zn1	0.5000	0.5000	0.7500	0.0075(2)
N1	0.65176(14)	0.65176(14)	0.7500	0.0108(4)
C1	0.66958(17)	0.73275(17)	0.81999(10)	0.0148(4)
Si1	0.5000	0.5000	0.5000	0.0089(3)
F1	0.5000	0.5000	0.61440(11)	0.0124(4)
F2	0.66683(13)	0.49224(13)	0.5000	0.0162(4)
$O1_X$	0.4599(6)	0.9599(6)	0.9230(4)	0.081(3)
$C1_X$	0.4612(10)	0.9612(10)	1.0000	0.067(4)
H1	0.6138	0.7226	0.8706	0.018

[a] Subscript x denotes CO_2 atoms.

Table S3. Anisotropic displacement parameters for CO_2-loaded SIFSIX-3-Zn

Atom[a]	u^{11}	u^{22}	u^{33}	u^{12}	u^{13}	u^{23}
Zn1	0.0080(3)	0.0080(3)	0.0065(3)	0.000	0.000	0.000
N1	0.0108(6)	0.0108(6)	0.0110(9)	-0.0007(7)	0.0004(5)	-0.0004(5)
C1	0.0159(9)	0.0169(9)	0.0117(7)	-0.0033(7)	0.0035(7)	-0.0014(7)
Si1	0.0108(4)	0.0108(4)	0.0051(6)	0.000	0.000	0.000
F1	0.0156(7)	0.0156(7)	0.0060(9)	0.000	0.000	0.000
F2	0.0115(7)	0.0255(8)	0.0117(7)	0.0003(5)	0.000	0.000
$O1_X$	0.102(5)	0.102(5)	0.039(3)	0.061(5)	0.009(2)	0.009(2)
$C1_X$	0.070(7)	0.070(7)	0.061(8)	0.049(7)	0.000	0.000

[a] Subscript x denotes CO_2 atoms.

Table S4. Bond lengths for CO_2-loaded SIFSIX-3-Zn[a]

Zn1-F1	2.0460(17)	Si1-F2[8]	1.6687(13)
Zn1-F1[1]	2.0460(17)	Si1-F2	1.6687(13)
Zn1-N1[2]	2.144(2)	Si1-F1[8]	1.7260(17)
Zn1-N1	2.144(2)	Si1-F1	1.7261(17)
Zn1-N1[3]	2.144(2)	$O1_X$-$O1_X$[9]	1.135(16)
Zn1-N1[4]	2.144(2)	$O1_X$-$C1_X$	1.162(5)
N1-C1[5]	1.3424(19)	$O1_X$-$C1_X$[10]	1.611(12)
N1-C1	1.3424(19)	$C1_X$-$C1_X$[10]	1.10(3)
C1-C1[6]	1.380(3)	$C1_X$-$O1_X$[11]	1.162(5)
C1-H1	0.9500	$C1_X$-$O1_X$[10]	1.611(12)
Si1-F2[7]	1.6687(13)	$C1_X$-$O1_X$[9]	1.611(12)
Si1-F2[4]	1.6687(13)		

[a] Subscript x denotes CO_2 atoms.

1. 1-x, y,1+ -z+1/2
2. 1-x,1+ -y, z
3. y,1+ -x, z
4. 1-y, x, z
5. y, x,1+ -z+1/2
6. 1-y+1/2,1+ -x+1/2, z
7. y,1+ -x,1+ -z
8. 1-x,1+ -y,1+ -z
9. 1-x,2+ -y, z
10. 1-x,2+ -y,2+ -z
11. x, y,2+ -z

Table S5. Bond angles for CO_2-loaded SIFSIX-3-Zn

F1[1]-Zn1-F1	180.0	F2[4]-Si1-F2	90.001(1)
F1[1]-Zn1-N1[2]	90.000(1)	F2[8]-Si1-F2	180.0
F1-Zn1-N1[2]	90.000(1)	F2[7]-Si1-F1[8]	90.0
F1[1]-Zn1-N1	90.000(1)	F2[4]-Si1-F1[8]	90.0
F1-Zn1-N1	90.000(1)	F2[8]-Si1-F1[8]	90.0
N1[2]-Zn1-N1	180.0	F2-Si1-F1[8]	90.0
F1[1]-Zn1-N1[3]	90.0	F2[7]-Si1-F1	90.0
F1-Zn1-N1[3]	90.0	F2[4]-Si1-F1	90.0
N1[2]-Zn1-N1[3]	90.000(8)	F2[8]-Si1-F1	90.0
N1-Zn1-N1[3]	90.000(8)	F2-Si1-F1	90.0
F1[1]-Zn1-N1[4]	90.0	F1[8]-Si1-F1	180.0
F1-Zn1-N1[4]	90.0	Si1-F1-Zn1	180.0
N1[2]-Zn1-N1[4]	90.000(8)	$O1_X^9$-$O1_X$-$C1_X$	89.1(9)
N1-Zn1-N1[4]	90.000(8)	$O1_X^9$-$O1_X$-$C1_X^{10}$	46.2(4)
N1[3]-Zn1-N1[4]	180.0	$C1_X$-$O1_X$-$C1_X^{10}$	42.9(12)
C1[5]-N1-C1	117.3(2)	$C1_X^{10}$-$C1_X$-$O1_X^{11}$	90.9(9)
C1[5]-N1-Zn1	121.34(10)	$C1_X^{10}$-$C1_X$-$O1_X$	90.9(9)
C1-N1-Zn1	121.34(10)	$O1_X^{11}$-$C1_X$-$O1_X$	178.2(18)
N1-C1-C1[6]	121.34(10)	$C1_X^{10}$-$C1_X$-$O1_X^{10}$	46.2(4)
N1-C1-H1	119.3	$O1_X^{11}$-$C1_X$-$O1_X^{10}$	44.8(7)
C1[6]-C1-H1	119.3	$O1_X$-$C1_X$-$O1_X^{10}$	137.1(12)
F2[7]-Si1-F2[4]	180.0	$C1_X^{10}$-$C1_X$-$O1_X^9$	46.2(4)
F2[7]-Si1-F2[8]	90.000(1)	$O1_X^{11}$-$C1_X$-$O1_X^9$	137.1(12)
F2[4]-Si1-F2[8]	90.000(1)	$O1_X$-$C1_X$-$O1_X^9$	44.8(7)
F2[7]-Si1-F2	89.999(1)	$O1_X^{10}$-$C1_X$-$O1_X^9$	92.3(9)

[a] Subscript x denotes CO_2 atoms.

1. 1-x, y,1+ -z+1/2

2. 1-x,1+ -y, z

3. y,1+ -x, z

4. 1-y, x, z

5. y, x,1+ -z+1/2

6. 1-y+1/2,1+ -x+1/2, z

7. y,1+ -x,1+ -z

8. 1-x,1+ -y,1+ -z

9. 1-x,2+ -y, z

10. 1-x,2+ -y,2+ -z

11. x, y,2+ -z

Table S6. Torsion angles for CO_2-loaded SIFSIX-3-Zn

$C1^1$-N1-C1-$C1^2$	-0.001(0)	$O1_X^3$-$O1_X$-$C1_X$-$O1_X^4$	0.000(3)
Zn1-N1-C1-$C1^2$	180.0	$C1_X^4$-$O1_X$-$C1_X$-$O1_X^4$	0.000(0)
$O1_X^3$-$O1_X$-$C1_X$-$C1_X^4$	0.000(1)	$C1_X^4$-$O1_X$-$C1_X$-$O1_X^3$	0.000(2)

[a] Subscript x denotes CO_2 atoms.

1. y, x,1+ -z+1/2
2. 1-y+1/2,1+ -x+1/2, z
3. 1-x,2+ -y, z
4. 1-x,2+ -y,2+ -z

Table S7. Potential hydrogen bonds for CO_2-loaded SIFSIX-3-Zn

Hydrogen Bond	D—H (Å)	H···A (Å)	D···A (Å)	D—H···A (°)
C1-H1···F1[1]	0.95	2.51	3.0429(18)	115.6
C1-H1···F2[2]	0.95	2.37	3.3091(17)	171.4

1. 1-x, y,1+ -z+1/2

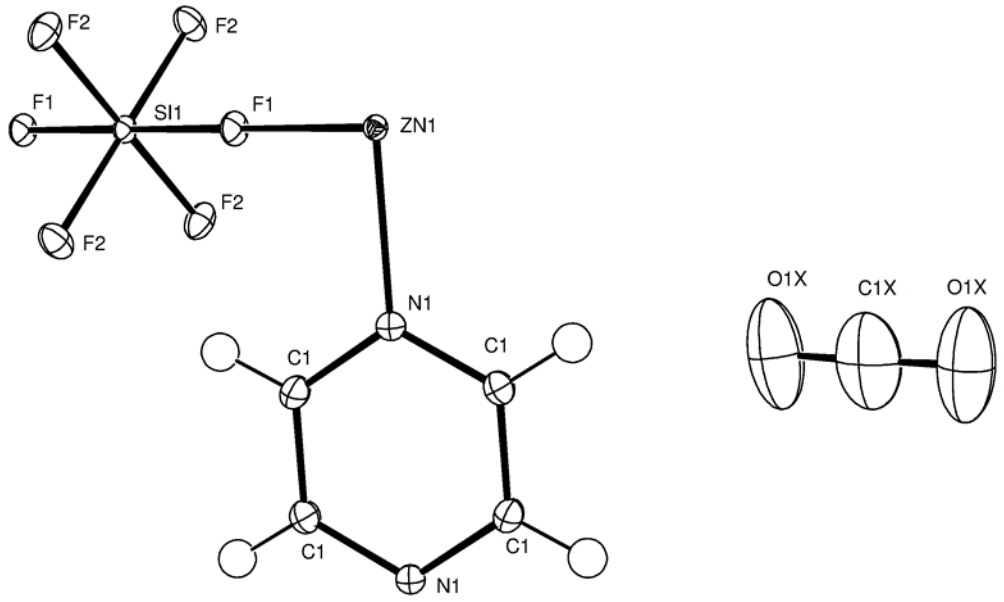

Figure S3. ORTEP drawing of CO_2-loaded SIFSIX-3-Zn molecular moieties. Ellipsoids are at the 50% probability level and hydrogen atoms were drawn with arbitrary radii for clarity.

Table S8. Comparison of angles (°) in as-made and CO_2-loaded SIFSIX-3-Zn.

	CO_2-loaded (110 K)	As-made (100 K)[2]	As-made (298 K)[1]
C-N-Zn	121.34(10)	121.86(14)	122.3(3)
C-N-C	117.3(2)	116.3(3), 111.1(3)	115.4(6)
C-C-H	119.3	119.100	118.900
F_{ax}-Zn-N	90.000(1)	90.000(1), 90.000	90.000(1), 90.000
F_{ax}-Zn-F_{ax}	180.0	180.000	180.000
F_{ax}-Si-F_{ax}	180.0	180.000	180.000
F_{eq}-Si-F_{ax}	90.0	90.000	90.000
F_{eq}-Si-F_{eq}	180, 90.000 (1), 89.999 (1), 90.001(1)	180.000, 90.000	180.000, 90.000
N-Zn-N	90.000(8), 180	90.000(1), 180.000	90.000(1), 180.000
N-C-H	119.3	119.100	118.900
N-C-C	121.34(10)	121.86(14)	122.3(3)
Si-F_{ax}-Zn	180.0	180.000	180.000

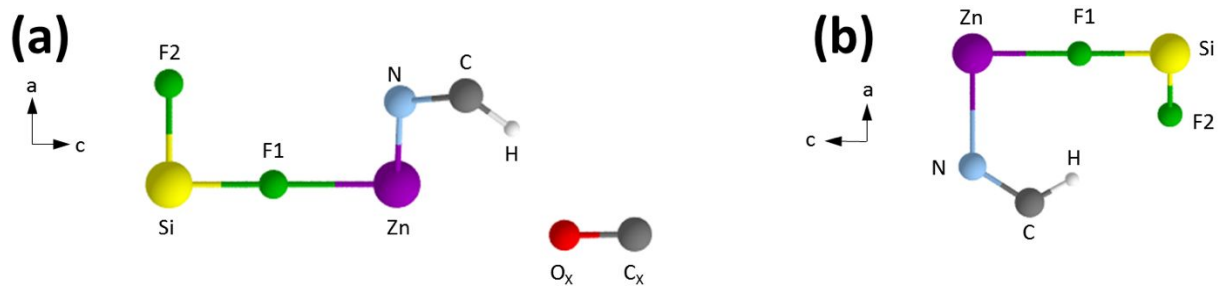

Figure S4. The asymmetric unit of (a) CO_2-loaded SIFSIX-3-Zn and (b) as-made SIFSIX-3-Zn[1], illustrating the number of crystallographically distinct Zn, F, C, H, and Si. Subscript x denotes CO_2 atoms in (a).

^{19}F and ^{29}Si SSNMR Results and Discussion

^{19}F MAS and ^{1}H →^{29}Si CP/MAS experiments were performed to probe the SiF_6^{2-} pillars and pyrazine (pyr) ligands. The ^{19}F MAS spectra are provided in Figure S5, and the experimental $\delta_{iso}(^{19}F)$ values of SiF_6^{2-} are summarized in Table S9. All three frameworks gave two distinct ^{19}F resonances: an intense resonance at ca. -131 ppm and a weak resonance at ca. -150 ppm. The presence of two resonances is consistent with the crystal structures of as-made and CO_2-loaded SIFSIX-3-Zn (Figure S4), which indicate that the F_{eq} and F_{ax} atoms in SiF_6^{2-} each have one crystallographically distinct site. Based on the 2:1 integration of the resonances, the more intense peak is assigned to the four F_{eq} atoms, while the less intense peak is assigned to the two F_{ax} atoms. Furthermore, the position of the $^{19}F_{eq}$ resonance of CO_2-loaded SIFSIX-3-Zn is slightly shifted (ca. 1 ppm) with respect to that of the as-made framework (Table S9), reflecting the structural differences between the two. On the other hand, the ^{19}F MAS spectrum of CO_2-loaded SIFSIX-3-Zn is comparable to that of the activated sample, indicating that the fluorine atoms reside in similar chemical environments.

The ^{1}H →^{29}Si CP/MAS SSNMR spectra are provided in Figure S5. One signal at ca. 185 ppm was detected in each spectrum, corresponding to the presence of one crystallographically distinct silicon site (Figure S4). The δ_{iso}(Si) values are similar to the values obtained in previous NMR studies of SiF_6^{2-}.[3] Furthermore, the CO_2-loaded sample has a δ_{iso}(Si) value comparable to that of the activated sample, but slightly different from that of the as-made sample (Table S9). Our ^{29}Si, ^{19}F and ^{67}Zn SSNMR results therefore all indicate that CO_2-loaded and activated SIFSIX-3-Zn have similar framework structures.

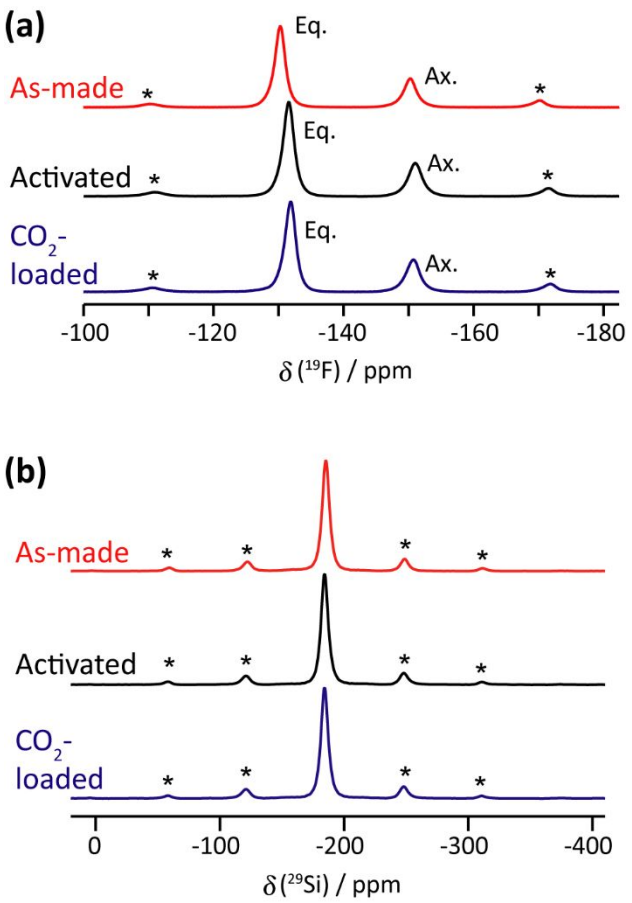

Figure S5. The (a) ^{19}F MAS and (b) $^{1}H \rightarrow {}^{29}Si$ CP/MAS SSNMR spectra of as-made (red trace), activated (black trace) and CO_2-loaded (blue trace) SIFSIX-3-Zn. All spectra were recorded at 9.4 T. Asterisks denote spinning sidebands.

Table S9. Experimental $\delta_{iso}(^{19}F)$ and $\delta_{iso}(^{29}Si)$ values of the SiF_6^{2-} pillars in as-made, activated, and CO_2-loaded SIFSIX-3-Zn.

Sample	**$\delta_{iso}(^{19}F)$ SiF_6^{2-} [ppm]**		**$\delta_{iso}(^{29}Si)$ SiF_6^{2-}[ppm]**
	F_{eq}	**F_{ax}**	
As-made	-130.3 (1)	-150.3 (1)	-185.5 (2)
Activated	-131.6 (1)	-151.0 (1)	-184.4 (2)
CO_2-loaded	-131.8 (1)	-150.8 (1)	-184.4 (2)

The Influence of Temperature on CO_2 Motional Rates in SIFSIX-3-Zn

Figure S6 shows the simulated static ^{13}C spectra for CO_2 in SIFSIX-3-Zn using a wobbling angle of 10°. The experimental spectrum acquired at 153 K is successfully simulated when a motional rate of $\geq$ ca. 10^6 Hz is used. Therefore, CO_2 wobbles at an angle of 10° at a rate $\geq$ ca. 10^6 Hz at 153 K. At higher temperatures, the experimental ^{13}C powder pattern lineshapes decrease in breadth (Figure 7). This could be due to an increase in motional rates. However, simulations show that further increase in rate to greater than 10^6 Hz does not result in any spectral changes (Figure S6), and the breadth of the ^{13}C powder pattern only decreases when the wobbling angle is altered. Thus, the observed experimental ^{13}C lineshape changes at higher temperatures are due to changes in motional angle instead of motional rate.

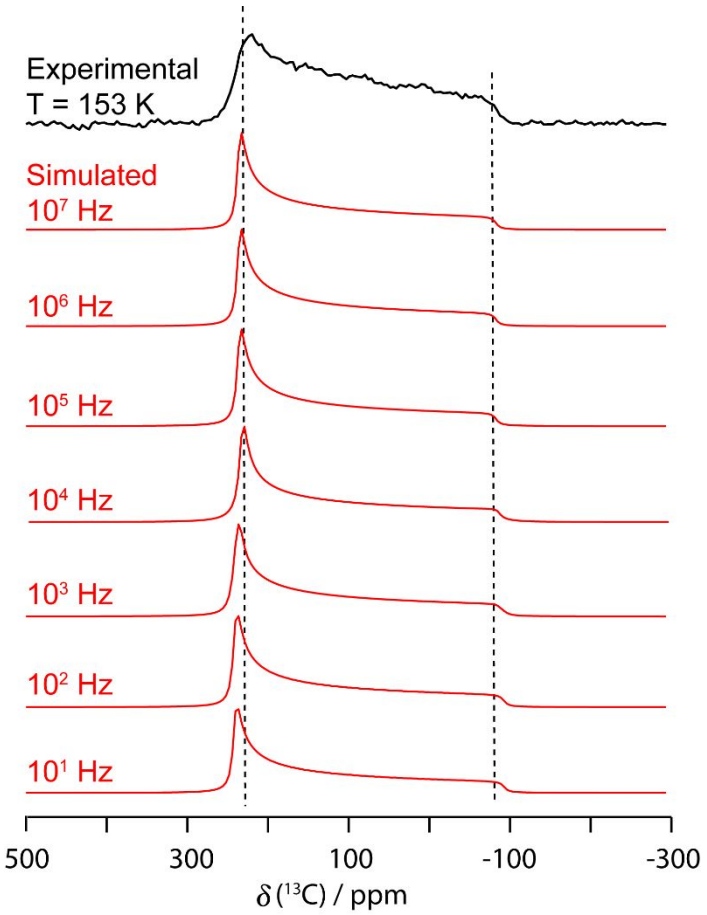

Figure S6. The experimental static ^{13}C SSNMR spectrum recorded for $^{13}CO_2$ in SIFSIX-3-Zn at 153 K (black) and the simulated static ^{13}C SSNMR spectra generated using a C_3 rotation (i.e., wobble) with a motional angle of 10° at various rates (red). The dashed lines serve as a guide to show changes in the apparent Ω and κ

References

(1) Uemura, K.; Maeda, A.; Maji, T. K.; Kanoo, P.; Kita, H. Syntheses, Crystal Structures and Adsorption Properties of Ultramicroporous Coordination Polymers Constructed from Hexafluorosilicate Ions and Pyrazine. *Eur. J. Inorg. Chem.* **2009,** *2009,* 2329-2337.

(2) Forrest, K. A.; Pham, T.; Hogan, A.; McLaughlin, K.; Tudor, B.; Nugent, P.; Burd, S. D.; Mullen, A.; Cioce, C. R.; Wojtas, L.; Zaworotko, M. J.; Space, B. Computational Studies of CO_2 Sorption and Separation in an Ultramicroporous Metal–organic Material. *J. Phys. Chem. C* **2013,** *117,* 17687-17698.

(3) Hoffner, F. M.; Delmotte, L.; Kessler, H. A $^{19}F/^{29}Si$ CP MAS N.M.R. Study of Microporous Solids Synthesized in Fluoride Medium. *Zeolites* **1993,** *13,* 60-63.